DYNA
http://dyna.medellin.unal.edu.co/

UNIVERSIDAD NACIONAL DE COLOMBIA

Detecting RFID chipless technology with software programmed radio: a study of slit and line configurations

Henry Mancini & Lauro Paulo da Silva Neto

UNIFESP - Universidade Federal de S. Paulo, São Paulo, Brazil. henry.mancini@unifesp.br, lauro.paulo@unifesp.br

Received: May 28th, 2023. Received in revised form: October 12th, 2023. Accepted: October 23th, 2023.

Abstract
The aim of this study was to investigate the potential for monitoring chipless RFID technology using a radio transmitter and receiver. The researchers analyzed the behavior of a printed label made with an aluminum-based ink from a thermal printer and compared the read characteristics of the receptor with a baseline. The results showed a shift in the reading characteristics near the resonance point of the curve. In the resonance area, the coded signal deviated from the baseline, floating above the baseline in the slit configuration and below in the line configuration. These observations provide valuable insights into the performance of chipless RFID technology and the potential to optimize its functionality. Chipless RFID technology has the potential to revolutionize the packaging industry by offering a cost-effective and efficient means of tracking and managing inventory. Unlike traditional RFID tags, chipless RFID utilizes the unique characteristics of the packaging material itself to store and transmit data, eliminating the need for expensive chips and simplifying the manufacturing and assembly process. Real-time item tracking, product quality and safety monitoring, and improved supply chain management are among the benefits of chipless RFID, with the potential to enhance efficiency, reduce waste, and increase profitability for companies.

Keywords: RFID chipless; thermal printing; resonators.

Detección de tecnología RFID sin chip con radio programada por software: un estudio de configuraciones de líneas y hendiduras

Resumen
El objetivo de este estudio fue investigar el potencial para monitorear la tecnología RFID sin chip usando un transmisor y receptor de radio. Los investigadores analizaron el comportamiento de una etiqueta impresa hecha con una tinta a base de aluminio de una impresora térmica y compararon las características de lectura del receptor con una línea de base. Los resultados mostraron un cambio en las características de lectura cerca del punto de resonancia de la curva. En el área de resonancia, la señal codificada se desvió de la línea de base, flotando por encima de la línea de base en la configuración de rendija y por debajo en la configuración de línea. Estas observaciones brindan información valiosa sobre el rendimiento de la tecnología RFID sin chip y el potencial para optimizar su funcionalidad. La tecnología RFID sin chip tiene el potencial de revolucionar la industria del empaque al ofrecer un medio rentable y eficiente para rastrear y administrar el inventario. A diferencia de las etiquetas RFID tradicionales, la RFID sin chip utiliza las características únicas del propio material de embalaje para almacenar y transmitir datos, eliminando la necesidad de costosos chips y simplificando el proceso de fabricación y ensamblaje. El seguimiento de artículos en tiempo real, la calidad del producto y el control de la seguridad, y la gestión mejorada de la cadena de suministro se encuentran entre los beneficios de RFID sin chip, con el potencial de mejorar la eficiencia, reducir el desperdicio y aumentar la rentabilidad de las empresas.

Palabras clave: RFID chipless; impresión térmica; resonadores.

1. Introduction

As we move further into the Fourth Industrial Revolution and prepare for the widespread deployment of 5G, the development of low-cost sensors is becoming increasingly important. In this drive for innovation, RFID chipless technology has emerged as a promising alternative to traditional, expensive silicon chips. It has been shown to offer

How to cite: Mancini, H. and Neto, L.P.S., Detecting RFID chipless technology with software programmed radio: a study of slit and line configurations. DYNA, 90(229), pp. 114-120, October - December, 2023.

cost-effectiveness and robustness, making it attractive for various applications. According to Liu [1], RFID chipless technology can improve food supply chain management through the tracking of food products. Li [2] has demonstrated its potential for real-time patient monitoring. Singh [3] also highlights its potential integration into smart city transportation systems for improved traffic flow.

In this study, we aim to demonstrate the capabilities of off-the-shelf technology [4] in detecting and characterizing RFID chipless geometries using a Radio Programmed by Software-SDR. Through comparison with electromagnetic simulations, we will examine the behavior of the S21 curve in both line and slit configurations in an open field setting. The potential for RFID chipless technology is enormous, offering new ways for innovation and the ability to transform the way process management such as food supply chains, patient health and smart city transportation [1].

The use of programmable radio technology has gained importance in recent years due to its versatility and flexibility. Software-Defined Rradio (SDR) technology enables users to modify and customize the radio's operating parameters, making it an ideal solution for various applications, including telecommunications, military communications, and industrial and commercial applications. One of the advantages of programmable radio technology is the its ability to support multiple frequency bands and communication standards, making it a versatile and flexible solution.

Another advantage of programmable radios is their ability to be reconfigured remotely, making them suitable for use in remote or difficult-to-access locations. They can also be updated with new software or firmware to add new features or correct any issues. In this study, programmable radio technology was used to measure the S21 information of RFID chipless geometries in an open field setting.

Overall, this study provides valuable insights into the accuracy and effectiveness of simulation software in predicting the behavior of antenna systems in real-world scenarios. The use of programmable radio technology, particularly SDR technology, has significant potential in various applications and can be a versatile and flexible solution for different communication standards and frequency bands. As technology continues to advance, it is likely that the use of programmable radio technology will become increasingly prevalent in various industries.[2]

2. Methodology

The study presented here focused on the comparison of the accuracy and effectiveness of simulation software to the behavior of antenna systems in real-world scenarios. The resonance points in frequencies from L1 to L5 (the tag configured as “line” – please refer to figure 1) were simulated using electromagnetic software, and the results were compared to actual readings taken in an open field environment using a quadripolar antenna setup (Figure 2). The coherence of the simulations and measurements was assessed, and the comparison provided valuable insight into the accuracy of the simulation software.

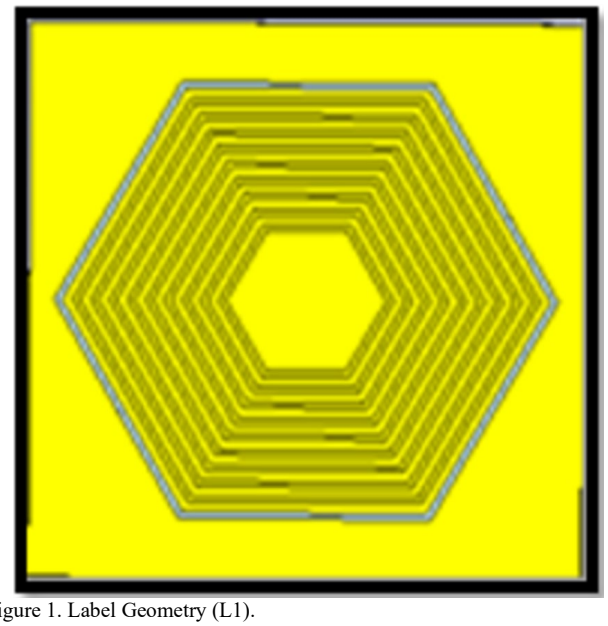

Figure 1. Label Geometry (L1).
Own Source, 2022.

Figure 2. Test Setup.
Own Source, 2022.

There were made at least 74 measurements of each tag for each given frequency in step of 0,01 GHz in the range of 0 to 3GHz and an average value was obtained from the measurements (from each given frequency step). The SDR used in this test was Great Scott Gadget HackRF One. The

antennas used in this test were Aquario Quadri band for cell phone CF-4000. We have not made any statistical assessment of our data since the data collected was a result of a 74 measurements average for each frequency step. We have confirmed empirically the repeatability of the values in different tests. All tests were performed in an indoor open environment. After the test completion, the data was extracted and plotted in MATLAB version 2020.

Measurements were taken considering the "line" label configuration and investigated which resonant region the curve rises above the baseline configuration (with fully substrate without any metallic ink printing). Similarly, in the "slit" configuration, a region will emerge where the encoded curve will be below the baseline (in this case, the fully substrate printed with metallic ink). These aspects constitute the main differences the two configurations while the geometry is basically the same.

The antennas used in these tests are regular quadripolar antennas CF-4000, commonly used for cellular signal amplification, with gains of 12 dBs in the bandwidth of 800 MHz to 3 GHz.

In the simulation (Figure 3), we will note at about 1.19 GHz, there will be a resonance point . The simulation was done in a electromagnetic simulator software for each label and using a bi-static antenna configuration and the result is related to a S21. The resonance area is coherent to the frequency of resonance as defined by the equation [4], where c is the speed of light and εr is the relative permittivity of the substrate and L0 is a physical length of the geometric resonator.

$$f_r = \frac{c}{2Lo\sqrt{\frac{2}{1+er}}} \qquad [4]$$

3. Results and Discussion

An SDR (Software Defined Radio) can help detect RFID chipless tags by demodulating the radio frequency signals that are emitted by the tags. By using software to process the signals, the SDR can extract information about the tags, such as their unique identification numbers. This information can then be used to determine the location and identity of the tagged objects.

To detect chipless RFID tags specifically, the SDR must be configured to receive signals at the right frequency and modulation scheme used by the tags.

Looking at Figure 3, we can see that in from 1 GHz to the 1.4 GHz the red line was positioned below the baseline (blue line). We can observe at about the surroundings of the resonance point indicated in the simulation; the red line is positioned slightly below the baseline.

Firstly, we will explain the label in the measured data. Looking at Figure 4, BLD60P40M1T means baseline measured at 60 cm, with radio calibrated with power 40dBM. Likewise, the acronym L1D60P40M1T means line1 measured at 60 cm, with radio calibrated with power 40dBM. Since there were many measured to determine the pattern T reflected the number of measurements that was selected.

We can observe the behavior is still the same with a slight difference. The larger difference between the L2 and baseline is 1.3GHz. There is still a difference between 1.1 GHz and 1.6 GHz, but it is evident the resonance area is moving gradually to a higher frequency. This is consistent to the simulation as shown in Figure 5 and Figure 6.

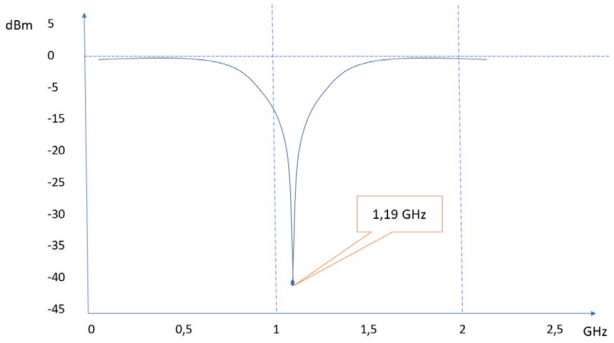

Figure 3. Line 3 Simulation - Resonance at 1.19 GHz.
Own Source, 2022.

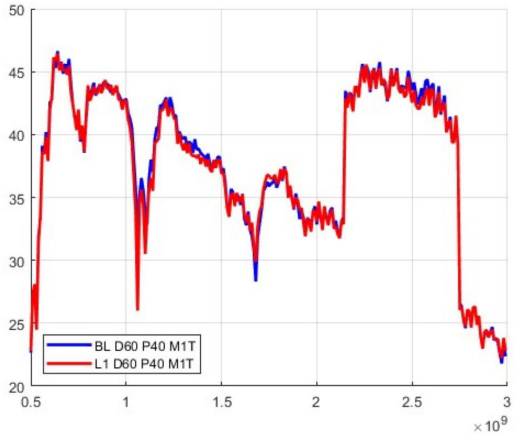

Figure 4. S21 printed L1 tag vs S21 baseline.
Own Source, 2022.

Again, the major difference between coded and baseline is located in 1.4 GHz (Figure 7). We can see there is a slight difference to the simulation that defines 1.5 GHz as the point of resonance, but this is still quite close and consistent to the simulation (Figure 8).

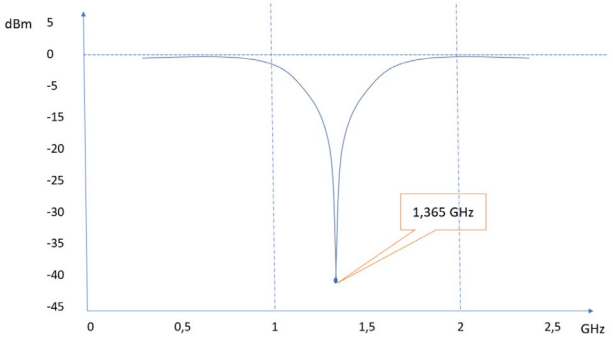

Figure 5. Line 2 Simulation - Resonance at 1.365 GHz.
Own Source, 2022.

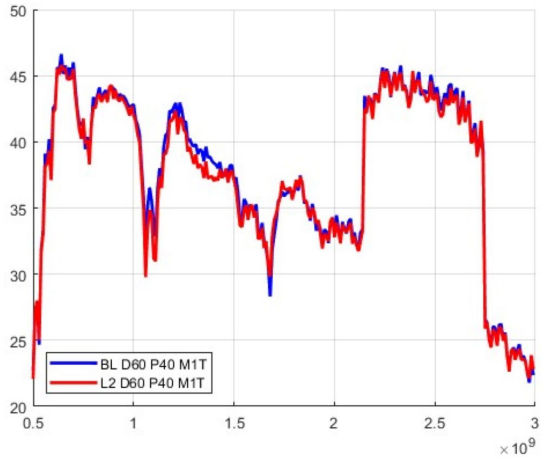

Figure 6. S21 printed L2 tag vs S21 baseline.
Own Source, 2022.

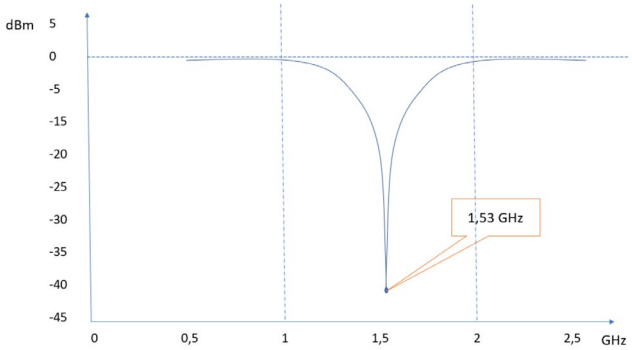

Figure 7. Line 3 Simulation - Resonance at 1.53 GHz.
Own Source, 2022.

For L4 and L5 (Figure 10 and 12), we can observe that the resonance area is not evident, even compared to the simulations (Figure 9 and 11).

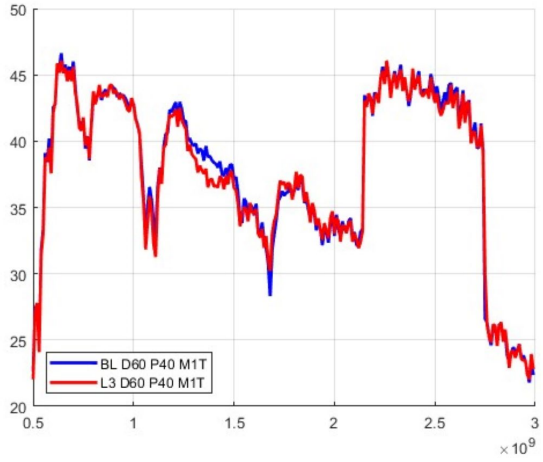

Figure 8. S21 printed L3 tag vs S21 baseline.
Own Source, 2022.

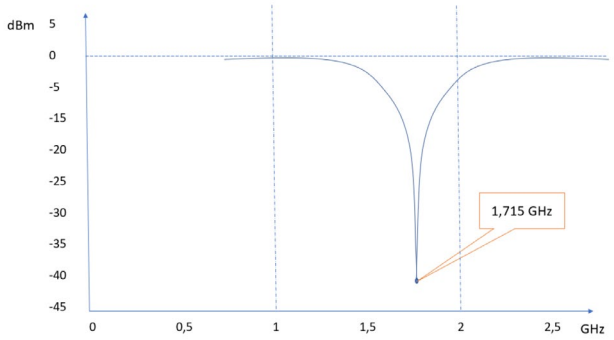

Figure 9. Line 4 Simulation - Resonance at 1.715 GHz.
Own Source, 2022.

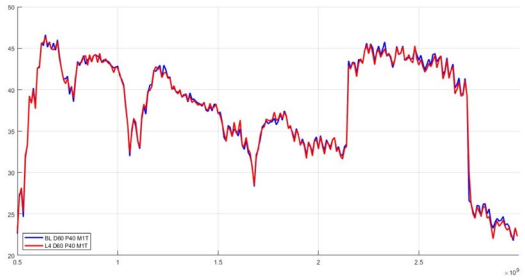

Figure 10. S21 printed L4 tag vs S21 baseline.
Own Source, 2022.

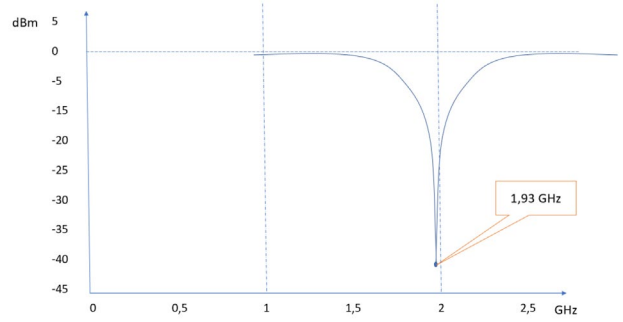

Figure 11. Line 5 Simulation - Resonance at 1.93 GHz.
Own Source, 2022.

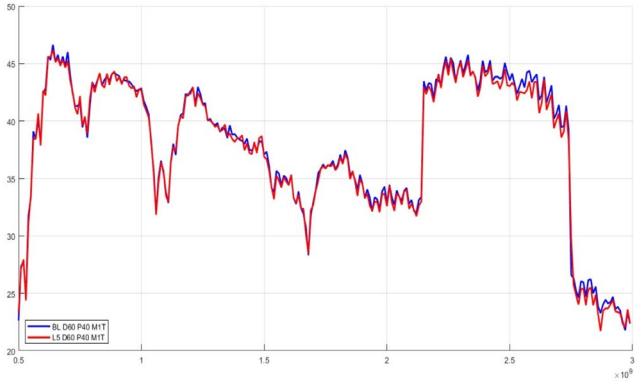

Figure 12. S21 printed L5 tag vs S21 baseline.
Own Source, 2022.

Next, we will compare the performance of the tag in slit configuration. In that setup, tag label will be printed fully with the metallic ink and the hexagon slit will be printed from SL1 to SL5. The larger slit represents the larger slit hexagon.

The baseline in this case, will be the background fully printed with metallic ink.

Note that at the S21 resonance surroundings, the S21 tag curve stays positioned above the baseline, which is totally consistent with the simulation. This pattern (that is reverse to the "line" configuration, where the tag line stayed below the baseline), remains consistent from SL1 to SL5.

We can clearly see that between 1 GHz and 1.5 GHz the coded line (red) is positioned above the baseline (blue). This is consistent with the simulation (Figures 13) that showed S21 peak is in about 1.2527 GHz.

At Figures 14, 16, 18, 20 and 22, we see that the resonance peak moves to the right as a pattern and this is consistent to the resonance peaks as shown in the simulations (Figures 13, 15, 17, 19 and 21).

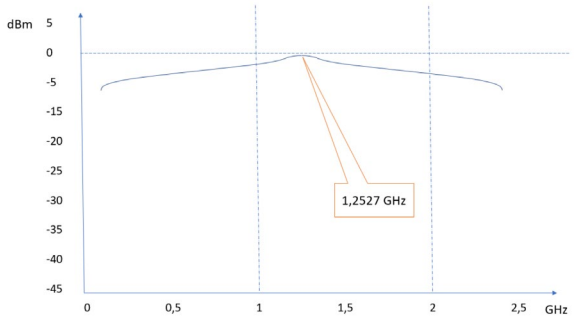

Figure 13. Slit 1 Simulation – S21 Resonance at 1.2527 GHz.
Own Source, 2022.

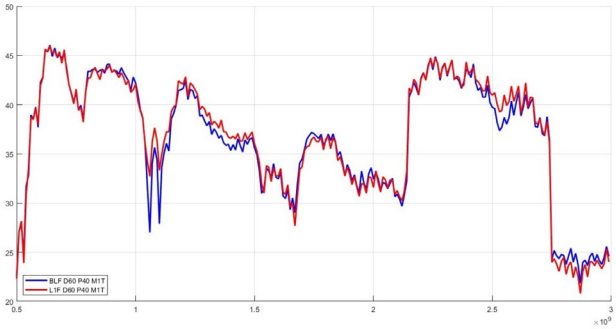

Figure 14. S21 printed SL1 tag vs S21 baseline.
Own Source, 2022.

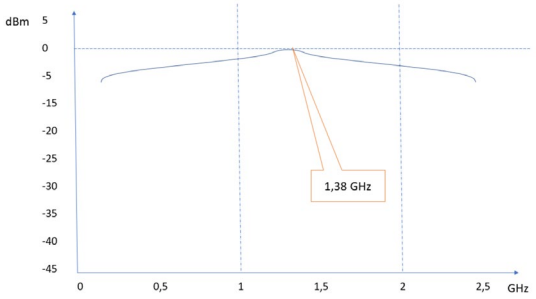

Figure 15. Slit 2 Simulation – S21 Resonance at 1.38 GHz.
Own Source, 2022.

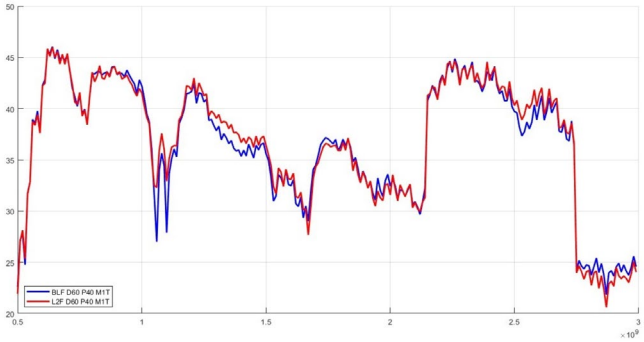

Figure 16. S21 printed SL2 tag vs S21 baseline.
Own Source, 2022.

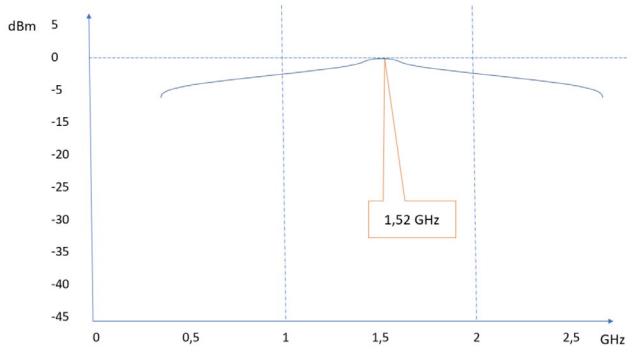

Figure 17. Slit 3 Simulation – S21 Resonance at 1.52 GHz.
Own Source, 2022.

At Figure 18 the same pattern is repeated while the resonance peak is moving rightwards, always compatible with the simulation that displayed the peak at 1.52 GHz.

And finally, on all measurements, the pattern is repeated. The peak is positioned in about 1.7 GHz what is compared to the simulation. Note that at the 1GHz, the difference between baseline and coded line is irrelevant. We see some small differences at 2.5 GHz, but this is attributed to the reflection in the open measurement. It was verified consistency of the measurement in all cases. To this article, we have selected the first measurement of each tag. The legend of the graphics of the tests indicates the parameters described above.

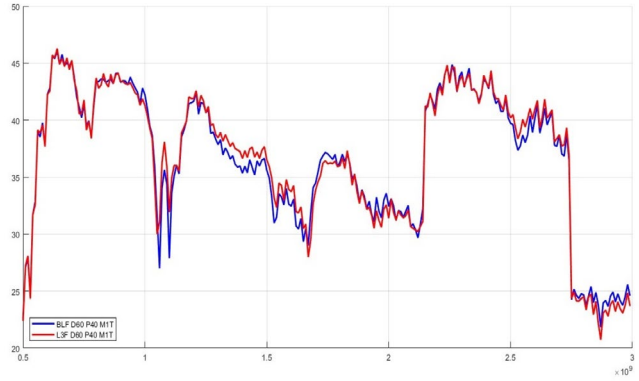

Figure 18. S21 printed SL3 tag vs S21 baseline.
Own Source, 2022.

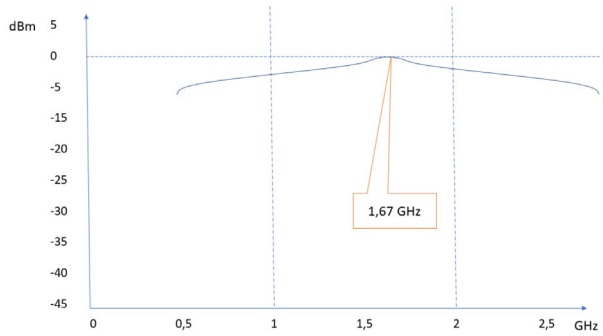

Figure 19. Slit 4 Simulation – S21 Resonance at 1.67 GHz
Own Source, 2022.

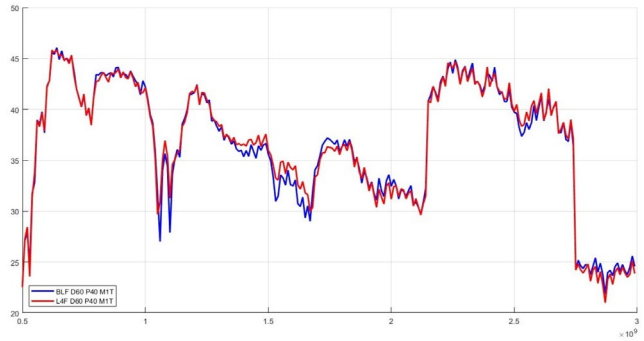

Figure 20. S21 printed SL4 tag vs S21 baseline.
Own Source, 2022.

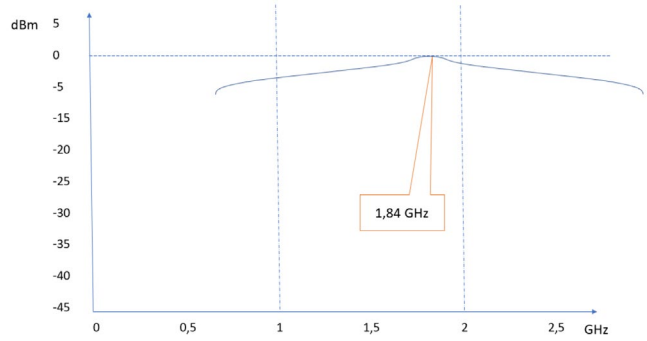

Figure 21. Slit 5 Simulation – S21 Resonance at 1.84 GHz.
Own Source, 2022.

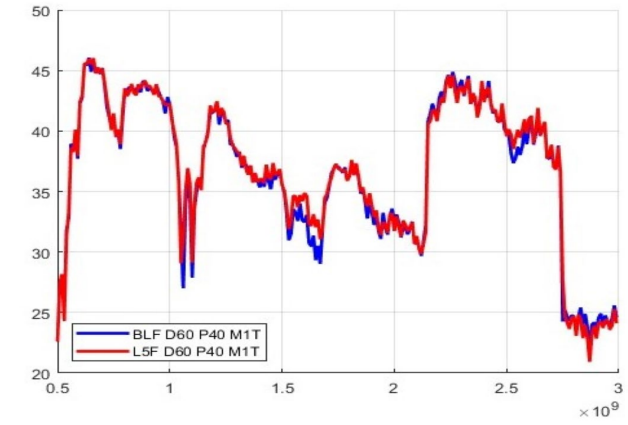

Figure 22. S21 printed SL5 tag vs S21 baseline.
Own Source, 2022.

Table 1.
Slit and Line configurations results

Tag characteristics	Line configuration	Slit Configuration
Tag baseline	Blank substrate with printed geometry in metallic ink	Fully printed substrate with metallic ink with slit geometry without metallic ink
S21 tag behavior compared to S21 baseline	Run below baseline	Run above baseline
Tag detection performance	For higher frequencies, the detection was not so evident	During the whole frequency band

Own Source, 2022.

In the table 1, we have described the performance for each configuration (slit and line) as an overview of the observations:

4. Conclusions

Radio-Frequency Identification (RFID) technology is rapidly gaining momentum in various industries, particularly in the 4.0 Industry as the world prepares for the large-scale introduction of 5G technology. One of the most promising advancements in this field is chipless RFID technology, which differs from traditional RFID in that it does not require a silicon chip to function. Instead, chipless RFID relies on printed labels, making it more cost-effective, robust, and versatile in its applications.

In this study, we aim to demonstrate how off-the-shelf technology can be used to detect and characterize a designed RFID chipless label and compare it to an electromagnetic simulation. Through open field tests, we aim to detail the behavior of the S21 curve in both slit and line configurations.

The results of our study show that in all cases of the "line" configuration, the tag curve is positioned below the baseline in the surrounds of the resonance point, as provided by simulation. This situation is reversed in the "slit" configuration, with the coded signal floating above the baseline around the resonance area.

Additionally, for the "line" configuration, the resonance areas were more detectable for lower frequencies, whereas for higher frequencies, the resonances were less detectable (L1 to L3). In contrast, it was possible to detect the resonance areas for "slit" configuration in all tags (from SL1 to SL5).

It is appropriate to say that the S21 approach, although is an indication of the label characterization, it consumes frequency band and other methods should be considered for tag codification. Traditionally with RCS technology [2] radar signals reflected by objects are analyzed to obtain valuable information about their size, shape, and material composition. This characterization is important for various applications such as military surveillance, object detection, and radar system design.

Our findings suggest that slit configuration is more appropriate for detecting the resonance due to the larger metallic ink area, resulting in a more evident signal-to-noise

ratio. Although our study has demonstrated the perception of a metallic inked print to a electromagnetic signature, much more has to be developed in order to make a codification of the information embedded in the tags such as filtering the resonance peaks in a thinner band (in order to codify more bits) and improve the overall reading environment.

Chipless RFID technology, which does not require a microchip to operate, has great potential in the industry due to its low cost, ease of deployment, and ability to track and monitor assets without physical contact. This can result in a revolutionary technology that can be suitable for a wide range of applications, including supply chain management, inventory control, and asset tracking.

References

[1] Singh, S. P. A. An RFID-based Intelligent Transportation System for Smart Cities, 2017.

[2] Wiesbeck, W. and Kahny, D., Single Reference, Three Target Calibration and Error Correction for Monostatic, Polarimetric Free Space Measurements. Proceedings of the IEEE [Online]. 79(10), pp. 1551-1558, 1991. DOI: http://www.doi.org/10.1109/5.104229

[3] Behera, S. K. and Karmakar, N. C., Chipless RFID Printing Technologies A State of Art. IEEE Microwave Magazine [Online]. 22(6), pp. 64-81, 2021. DOI: http://www.doi.org/10.1109/MMM.2021.3064099

[4] Karmakar, N., Eman, C. A. and Kumar, S. Chipless RFID sensors. New Jersey: John Wiley & Sons, 2016.

[5] Lee, Y. An RFID-based Inventory Management System for Retail Stores, Journal of Retailing and Consumer Services, 2020.

[6] Li, S. An RFID-based Monitoring System for Food Supply Chain Management, Journal of Food Science and Technology, 2016.

H. Mancini has Bs. Eng in Electronic Engineering in 1996, and MS in Innovation for Universidade Federal de SP in 2023.
ORCID: https://orcid.org/0000-0002-9591-3341

L. P. da Silva Neto is currently an Professor at the Federal University of São Paulo, São José dos Campos campus and a teaching member of the Postgraduate Professional Masters in Technological Innovation course. He holds a PhD and MS degree in Space Engineering and Technology (ETE) in concentration Engineering and Management of Space Systems (CSE) from INPE. Electrical Engineer (Electronics) title. Member of IEEE and Collaborator (Research) at the National Institute for Space Research (INPE). He has experience in Electronic Devices and Components area, having worked as a PCI fellow at the Telecommunications Engineering Laboratory in the Aerospace Electronics Division (DEA) of INPE from 2008 to 2009 (CBERS Project), and has experience with building electrical installations, acting as Electrical Engineer at the Federal University of São Paulo, São José dos Campos campus from 2013 to 2017.
ORCID: https://orcid.org/0000-0001-9862-4601